Biomedical Engineering Letters (2024) 14:199–207
https://doi.org/10.1007/s13534-023-00327-2

ORIGINAL ARTICLE

CIsense: an automated framework for early screening of cerebral infarction using PPG sensor data

Shresth Gupta[1] · **Anurag Singh**[1] · **Abhishek Sharma**[1]

Received: 16 June 2023 / Revised: 24 September 2023 / Accepted: 26 September 2023 / Published online: 16 October 2023

Abstract

A cerebral infarction (CI), often known as a stroke, is a cognitive impairment in which a group of brain cells perishes from a lack of blood supply. The early prediction and evaluation of this problem are essential to avoid atrial fibrillation, heart valve disease, and other cardiac disorders. Different clinical strategies like Computerized tomography (CT) scans, Magnetic resonance imaging (MRI), and Carotid (ka-ROT-id) ultrasound are available to diagnose this problem. However, these methods are time-consuming and expensive. Wearable devices based on photoplethysmography (PPG) are gaining prevalence in diagnosing various cardiovascular diseases. This work uses the PPG signal to classify the CI subjects from the normal. We propose an automated framework and fiducial point-independent approach to predict CI with sufficient accuracy. The experiment is performed with a publicly available database having PPG and other physiological data of 219 individuals. The best validation and test accuracy of 91.8% and 91.3% are obtained after diagnosis with Coarse Gaussian SVM. The proposed work aims to extract cerebral infarction pathology by extracting relevant entropy features from higher order PPG derivatives for the prediction of CI and offers a simple, automated and inexpensive approach for early detection of CI and promotes awareness for the subjects to undergo further treatment to avoid major disorders.

Keywords APPG · CI · Prediction · Entropy · JPPG · Sensor signal processing

1 Introduction

Strokes are regarded as one of the most dangerous medical conditions since they can cause lasting physical and mental consequences such as hemiparesis, ataxia, speech, vision or awareness impairment, and dementia. In severe situations, they can even be fatal. It is the second leading cause of death in the world, with a mortality rate of about 5.5 million per year [1].

An interruption in the blood flow to a part of the brain causes cerebral infarction, often known as an ischemic stroke. Lack of blood flow deprives brain cells of oxygen, causing cell ageing and poor brain function. Magnetic Resonance Imaging (MRI) and Computed Tomography (CT) are being employed extensively for its neurological diagnosis [2]. However, these still have limits in the examination process in terms of radiation exposure, hypersensitive responses, expensive costs, non-portable devices, and extended testing times. Studies are currently concentrating on non-invasive methods that are practical and portable in an effort to get over these constraints. The use of PPG signal, a low-cost method for detecting changes in blood volume in the micro-vascular bed of tissue, is growing popularity in continuous vital monitoring, early diagnosis of several medical conditions, and treatment of cardiovascular disease [3–7]. Researchers have created a number of non-invasive approaches for predicting disorders associated to CVD as a result of recent technological advancements. Numerous studies have employed Electrocardiogram (ECG) signal combined with PPG to predict stroke disorders. Stroke is frequently caused by atrial fibrillation (AF). It is known that silent CI can happen both with and without AF, however it is unclear how these two effects are related. Thus, a separate framework is required to diagnose CI to alert the subject regrading further treatment in clinic. J. Yu et al. [8] proposed a stroke disease diagnostic framework for elderly subjects using ensemble

✉ Shresth Gupta
shresth@iiitnr.edu.in

Anurag Singh
anurag2685@gmail.com

Abhishek Sharma
abhishek@iiitnr.edu.in

[1] IIIT Naya Raipur, Raipur, Chhattisgarh 493661, India

structure having CNN and LSTM combination. Fallet et al. dervied multiple statistical features of PPG like mean, standard deviation, and other inter-beat interval-based features and provided as inputs to the decision tree model [9]. Linda et al. used PPG and acceleration data acquired from wrist and used waveform features along with inter pulse interval features to diagnose CVD [10]. Another related work predicted both CI and diabetes mellitus using morphological features of PPG and utilized Fine Gaussian Multi class Support Vector Machine (FGMSVM) for classification [11]. The challenges associated with the manual feature extraction includes accurate detection of fiducial points from each PPG cycles. Further, the approach also requires an optimal filtering before feature extraction to remove unwanted noisy components that creates barrier in key-point detection. The limitations are resolved by the proposed framework for automatic prediction of CI by calculating the useful state-of-the-art entropy features calculated from a complete short recorded PPG episode instead of a single cycle. The key contribution of the proposed work are:

- Creating a reliable PPG preprocessing framework with a two-step filtering method to reduce artefacts in raw PPG in order to extract the clean PPG that is closest to the original in terms of morphology and preserve its clinically important points.
- Extraction of fiducial point independent state-of-the-art entropy features from second and third derivative of PPG called acceleration plethysmogram (APG) and Jerk PPG respectively [12] and utilization of these features for prediction using different machine learning classifiers.

2 Data source

The PPG-BP database, which is available to the public, contains 657 data records from 219 subjects is used for this study [14]. The database contains information for individuals aged between the ages of 20 and 89 as well as pathology for CI. The expected test parameters were followed in the data collecting process. At a frequency of 1 kHz, the PPG signal is recorded. Other significant vital parameters and demographic data of subjects, such as heart rate (HR), body mass index (BMI), age, sex, etc., are also present in the database in order to develop algorithms to forecast various cardiac and brain abnormalities like diabetes, cerebral infarction etc.

3 Methodology

The block diagram shown in Fig. 1 illustrates the pipeline of the proposed work. Pre-processing block performs necessary optimal filtering of the raw PPG corrupted with noise followed by a block that computes the second and third derivative of the clean PPG. These two PPG derivative sequence are fed to the entropy calculation block which calculates four state of the art entropy from these uni-variate sequence. The obtained entropy features are further given to machine learning classifiers which provides prediction results. The detailed methodology is provided in the below subsections.

3.1 Preprocessing of raw PPG records

Digital filtering is a critical step in minimising the impact of noise on PPG signal processing. Signal noise must be reduced in order to retrieve valuable information from PPG signals. Following a thorough study, we noticed that the majority of short recorded PPG episodes were corrupted, containing low amounts of motion artifacts and high frequency noise. We used a two step filtering approach in the preprocessing module to reduce these artefacts without impacting the clinical information from PPG. The brief explanation of both filtering steps are given below:

- A natural morphological form may be extracted from a raw noisy PPG that has been distorted by high frequency noise and small motion artefacts. In this stage, we are using Discrete Wavelet transform (DWT) and decompose

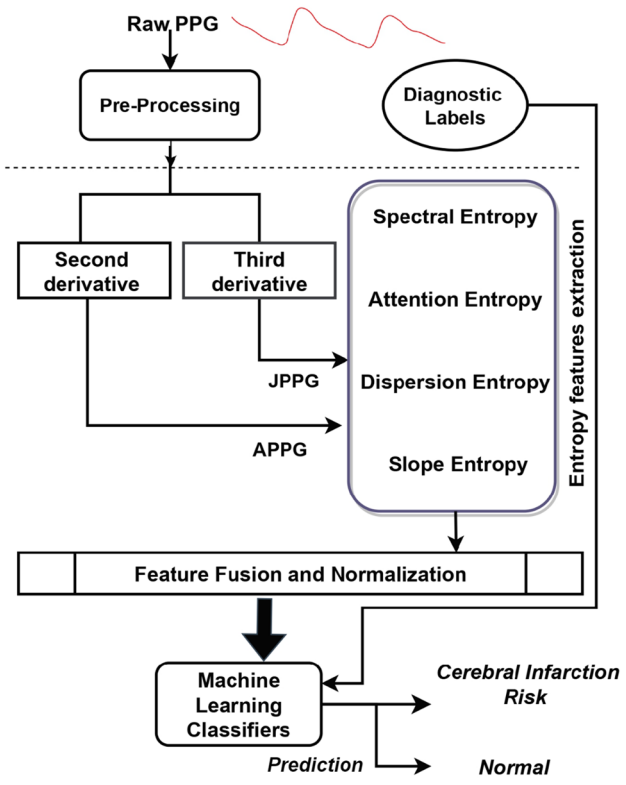

Fig. 1 Block diagram of the proposed automated framework for cerebral infarction prediction using raw PPG

the PPG signal using 12-level wavelet decomposition (using *db*8 mother wavelet) which produces coefficients for all of the PPG's frequency content. The high frequency noise coefficients are suppressed in the following phase, and the PPG is then rebuilt using the remaining coefficients [15].

- The Savitzky Golay (SG) filter is used to finish the smoothing in the next stage [16]. The signal-to-noise ratio of a series of digital data points is improved using the SG filter without deforming the signal. Convolution of all the polynomials is obtained after fitting the subsets of subsequent data points using a low order polynomial and the linear least squares method.

The filtered and refined PPG from each filtering steps with corresponding spectogram profile are demonstrated in Fig 2.

3.2 Extraction of PPG's higher order derivatives and its significance

A number of cutting-edge techniques have previously been investigated to extract useful characteristics from the natural PPG and its first derivative (VPPG) for applications including vascular ageing prediction and cuff-less blood pressure monitoring. After doing an experimental examination, we discovered that these PPG and VPPG signals had very limited capacity to deliver a significant pathology or discrimination between a normal and a subject with some complications like CVD, hypertension etc. It is already identified that the amplitude of a peak's n^{th} derivative is inversely proportional to the n^{th} power of its width for signals with the same form and amplitude. Because of this, differentiation effectively discriminates against peaks that are more prominent, and the discrimination becomes stronger as differentiation orders increase due to larger derivative significance [12]. With this motive we extracted the second and third derivative from our preprocessed clean PPG know as *APPG* and *JPPG* [13] as shown in Fig. 3. It is well indicated in the resultant waveforms that the natural clean PPG has a very simple morphological cycles which yields a very limited pathological information. On the other hand, the higher order PPG derivatives (APPG and JPPG) has sufficient randomness in their cycles to produce intrinsic pathological information in terms of entropy.

PPG cycles have increased variability in higher-order derivatives, which appears discriminatory for people with normal and CI conditions. Figure 4 shows the sample of PPG record plotted for both CI and normal class (after filtration) along with their third derivative (JPPG). It can be observed that the PPG in its natural form does not show much difference in its morphology while their JPPG's shows significant dynamic variations to motivate us towards the extraction of non-linear features for our classifier model in terms of state-of-the-art entropy.

3.3 Extraction of entropy features from APPG and JPPG

We have calculated four entropy attributes from each derivative sequence *APPG* and *JPPG* extracted from PPG records of both CI and normal category. The brief discussion and mathematical expression of the extracted entropy features are detailed below:

3.3.1 Spectral entropy

Spectral entropy is capable of calculating the spectral complexity of an uncertain system [17]. To calculate the spectral entropy of our PPG time series (x), we first need to calculate its power spectral density (PSD), which is a measure of the energy distribution of the signal over different frequencies. The PSD can be estimated using techniques such as the fast Fourier transform (FFT).

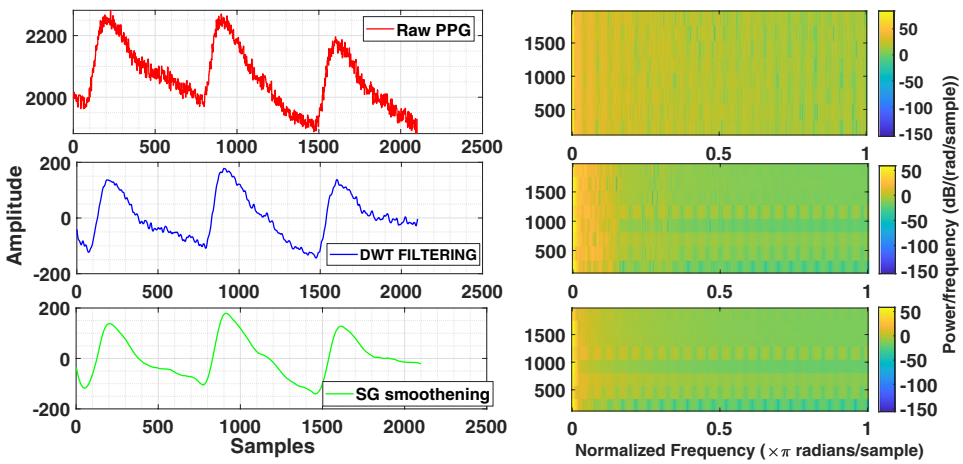

Fig. 2 Clean PPG obtained from the proposed two-step filtering approach and the corresponding spectrogram profile of the PPG in each stage

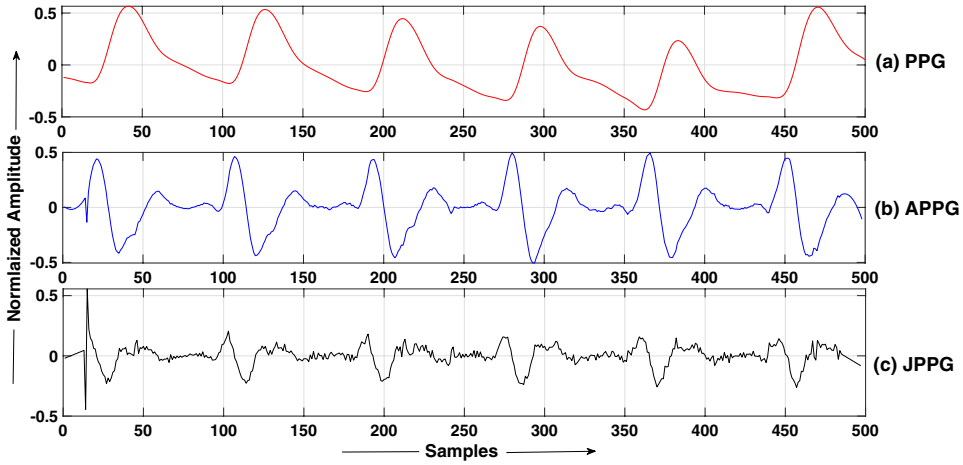

Fig. 3 Visualization of clean PPG obtained from proposed filtering approach and its second and third derivative

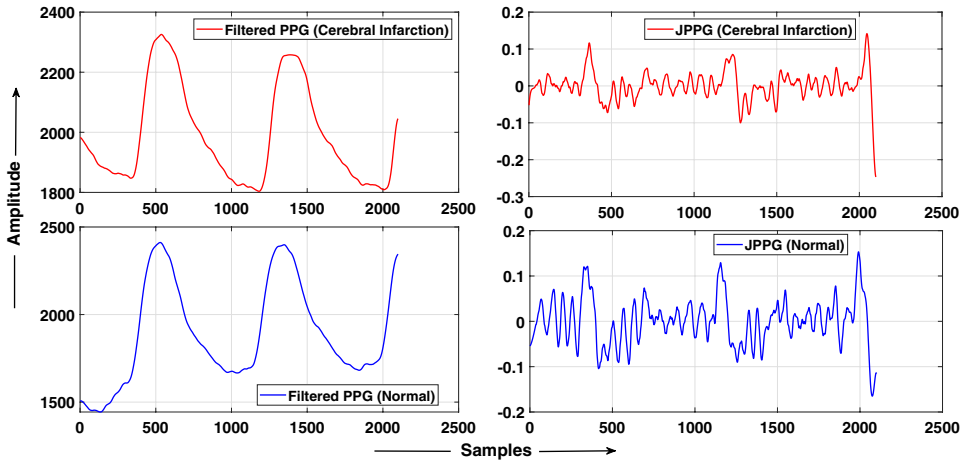

Fig. 4 A sample of PPG record plotted from each CI and normal class along with their third derivative (JPPG)

Once we have the PSD estimate, the spectral entropy (H) of our PPG time series (x) can be calculated using the following mathematical expression:

$$H = -\sum_{i=1}^{n} p_i \log_2(p_i) \tag{1}$$

where p_i is the normalized power spectral density at frequency i, and the summation is taken over all frequency bins. The calculation for spectral entropy calculation is explained in Algorithm 1.

Algorithm 1 Calculate Spectral Entropy for PPG Signal

procedure CALCULATESPECTRALENTROPY(x, segmentLength, f_s)
  numSegments $\leftarrow \lfloor \text{length}(x)/\text{segmentLength} \rfloor$
  entropySum $\leftarrow 0$
  for $i \leftarrow 0$ to numSegments $- 1$ **do**
    segment $\leftarrow x[i \times \text{segmentLength} : (i+1) \times \text{segmentLength}]$
    powerSpectrum $\leftarrow$ computePowerSpectrum(segment)
    entropy $\leftarrow$ computeEntropy(powerSpectrum)
    entropySum $\leftarrow$ entropySum $+$ entropy
  end for
  H $\leftarrow \frac{\text{entropySum}}{\text{numSegments}}$
  return spectralEntropy
end procedure

3.3.2 Attention entropy

Only the most important observations are taken into consideration by attention entropy. It evaluates the frequency distribution of the spaces between the important observations in a PPG time series rather than calculating the frequency of all observations. The following three stages are used to compute attention entropy: Identification of the key patterns, measurement of the distances between two adjacent key patterns, and measurement of the Shannon entropy of the interval [18]. For the given time series PPG **x** the attention entropy can be expressed as:

$$H = -\sum_{i=1}^{n} w_i \log_2(w_i) \tag{2}$$

where n is the length of the time series signal, and w_i is the normalized attention weight at time i, which measures the importance of the signal value at time i in the computation of the attention entropy.

The attention weight w_i is typically defined as a function of the similarity between the signal value at time i and the values of the neighboring time points. Different definitions of the attention weight can be used depending on the specific application.

3.3.3 Dispersion entropy

Dispersion entropy (DsEn) can recognise changes in frequency and amplitude while simultaneously detecting noise bandwidth for a given PPG sequence [19]. According to Shannon's concept of entropy, the following formula is used to determine the DsEn value with embedding dimension m, time delay k, and the number of classes c:

$$\begin{aligned}&\mathrm{DsEn}(\mathbf{x}, m, c, k)\\ &= -\sum_{\pi=1}^{c^m} d(\pi_{v_0 v_1 \ldots v_{m-1}}) \cdot \ln\left(d(\pi_{v_0 v_1 \ldots v_{m-1}})\right)\end{aligned} \tag{3}$$

where, $d(\pi_{v_0 v_1 \ldots v_{m-1}})$ indicates the number of dispersion patterns $\pi_{v_0 v_1 \ldots v_{m-1}}$ divided by the embedding dimension m.

3.3.4 Slope entropy

Slope entropy (SlEn) aims to include amplitude information into a purely symbolic representation of the given PPG episode. Based on the difference between successive samples of the input PPG time series, each symbol is allocated on the basis of symbolic pattern's relative frequency. The technique makes use of an alphabet consisting of the numbers 0, 1, and 2, as well as positive (+) and negative (-) variations of the last two. Each symbol represents a range of slopes for the segment connecting two successive samples of the input data, and a Shannon entropy technique is used to convert the relative frequency of each pattern recognized into a real number [20]. The necessary steps for the calculation of slope entropy from the PPG episode is provided in Algorithm 2.

Algorithm 2 Calculate Slope Entropy for PPG Signal

procedure CALCULATESLOPEENTROPY(x, segmentLength, threshold)
  numSegments $\leftarrow \lfloor \text{length}(x)/\text{segmentLength} \rfloor$
  entropySum $\leftarrow 0$
  for $i \leftarrow 0$ to numSegments $- 1$ **do**
    segment $\leftarrow x[i \times \text{segmentLength} : (i+1) \times \text{segmentLength}]$
    slopeValues $\leftarrow$ segment$[1:] -$ segment$[:-1]$
    pairCount $\leftarrow$ countPairs(slopeValues, threshold)
    probability $\leftarrow \frac{\text{pairCount}}{\binom{\text{segmentLength}}{2}}$
    segmentEntropy $\leftarrow -\text{probability} \times \log(\text{probability})$
    entropySum $\leftarrow$ entropySum $+$ segmentEntropy
  end for
  SlEn $\leftarrow \frac{\text{entropySum}}{\text{numSegments}}$
  return SlEn
end procedure

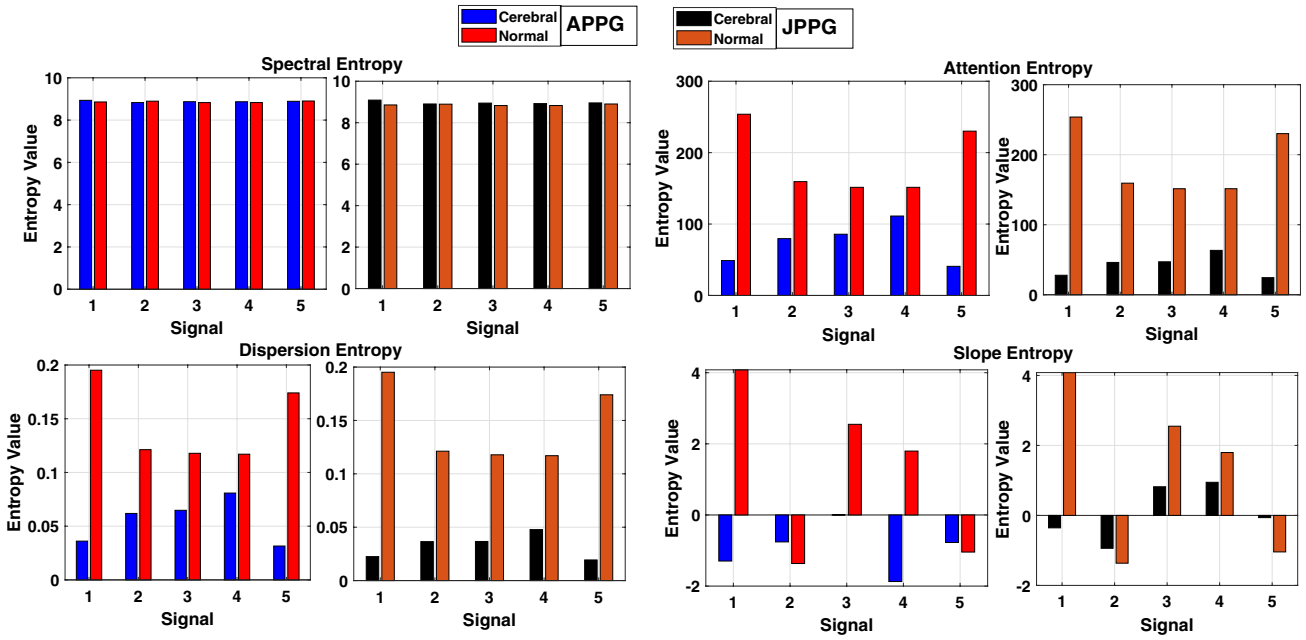

Fig. 5 Plot of entropy values calculated from APPG and JPPG of five PPG records taken from each CI and normal subjects

4 Results

To show the discrimination obtained in the entropy values calculated from APPG and JPPG, we took 5 PPG records each from CI and normal subjects and calculated their four entropies using the method described above. Figure 5 illustrates the difference in their entropy values in each class calculated from their APPG and JPPG. It is visible that JPPG indicates a higher potential of separating the two classes as the difference in all four entropy values is higher than the difference indicated by APPG. Further, amongst all these four entropies, the dispersion entropy shows the highest discrimination between the two classes, marking a significant difference between the entropy values followed by attention entropy and slope entropy. This analysis also indicates the contribution of individual entropy features and their significance towards better performance of the ML model in classification. Hence, we have also analyzed the feature importance score after the classification results in this section. The data set used in this work contains short PPG records and physiological data of 219 subjects. Each subject has three short-recorded PPG signals, which gives 657 PPG records. Of these subjects, 45 were found to have cerebral infarction and cerebrovascular disease. Thus, these 45 subjects contain $45 \times 3 = 135$ PPG records of CI in which one record with highly corrupted noise is removed. We have chosen 32 subjects labeled as normal and have no other medical conditions. It gives $32 \times 3 = 96$ PPG records. The combination of both these records gives 230 PPG records in which 10% records are separated for testing. The four different entropy features are calculated from the second and third derivatives of PPG, which gives eight entropy values (4

Table 1 Classification performance of popular machine learning classifiers for the prediction of CI

Model	Model hyperparameters	Validation accuracy (in %)	Test accuracy (in %)	Training time (in Sec)
Naive Bayes	Kernel type: Gaussian	91.3	87	50.02
KNN	Preset: Medium KNN No. of neighbors: 10 Distance metric: Euclidean	91.3	87	6.55
SVM	Preset: Coarse gaussian SVM Kernel function: Gaussian Kernel scale: 93	**91.8**	**91.3**	**4.77**

Coarse gaussian SVM secured highest classification accuracy compared to other two classifiers and hence it is highlighted in bold

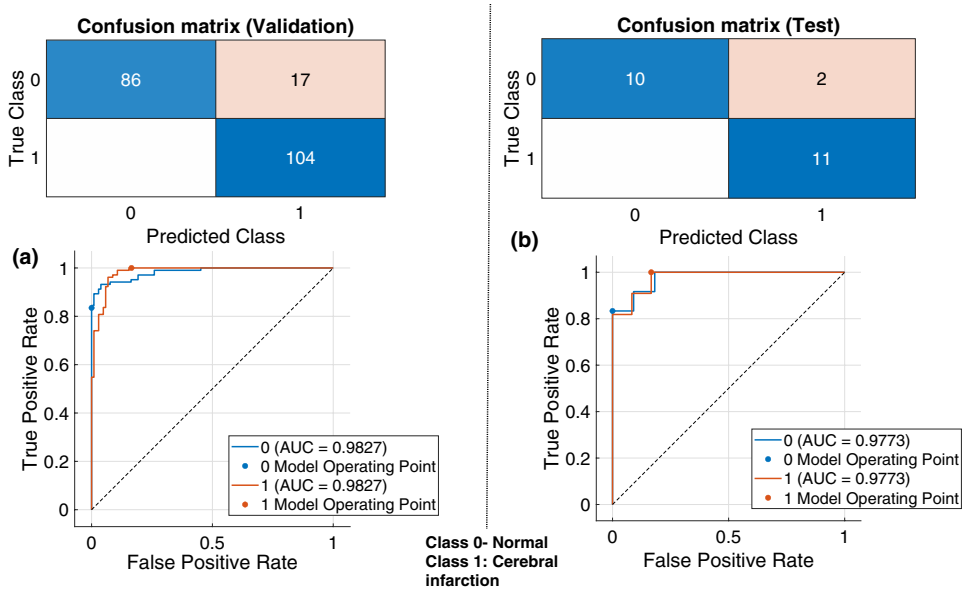

Fig. 6 Confusion matrix and AUC-ROC curve after classification using SVM **a** for validation data **b** for test data

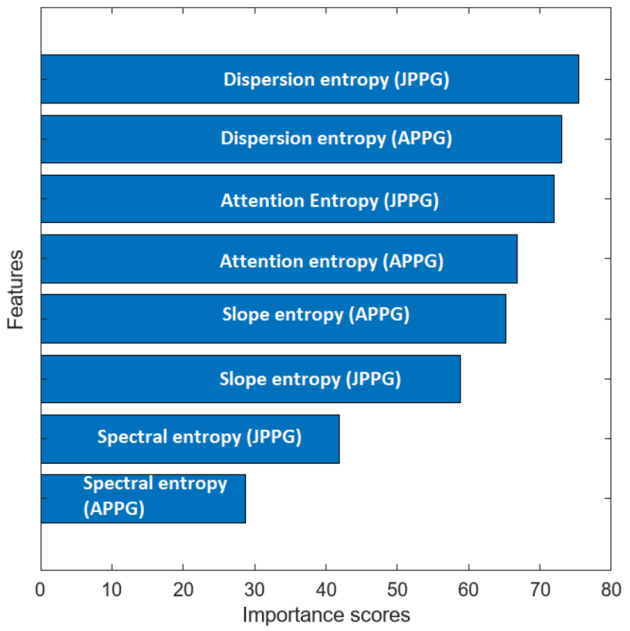

Fig. 7 Feature importance score sorted using Kruskal Wallis algorithm after classification with SVM

from each derivative). Thus, we got a feature dimension of 230×8 for training and validation. We utilized three popular machine learning classifiers to obtain the prediction. The obtained results are mentioned in Table 1.

The results reveal that support vector machine (SVM) outperformed the other two classifiers with highest validation and test accuracy of 91.8% and 91.3% respectively and also with training time of 4.77 Sec which is significantly

Table 2 Computational complexity of popular filtering approaches (N denotes the length of PPG signal while M denotes the size of the filter kernel or window)

Filtering approach	Computational complexity
Savitzky-golay filtering	$O(N \cdot M)$
DWT filtering	$O(N \cdot \log_2(N))$
Moving average (MA) filtering	$O(N \cdot M)$
Exponential moving average (EMA)	$O(N)$
Butterworth filter	$O(N \cdot M)$
Median filter	$O(N \cdot M \cdot \log_2(M))$
Kalman filter	$O(N)$
Fast Fourier transform (FFT)	$O(N \cdot \log_2(N))$

lower than Naive Bayes. A brief classification performance of our best performing model is illustrated in Fig. 6 in terms of confusion matrix and AUC-ROC curve. It can be seen in validation data that Normal class has no mis-classification while only 17 classes are mis-classified in class CI. In test data also only 2 mis-classification is found in CI class. Higher accuracy in both validation and test data indicates the potential of the proposed work to predict CI.

In order to evaluate the significance or contribution of each feature individually we performed Kruskal Wallis algorithm test to obtain feature importance score shown in Fig. 7. The Kruskal-Wallis test's null hypothesis is that the groups' mean rankings are identical. Kruskal-Wallis test is referred to as one-way ANOVA on ranks, the non-parametric alternative of one-way ANOVA.

The non-parametric Kruskal-Wallis test does not assume a normal distribution of the underlying data, in contrast to the comparable one-way ANOVA [21]. Out

Table 3 Computational complexity and key advantages of entropy calculation methods used in the proposed framework

Entropy calculation method	Computational complexity	Key advantage(s)
Spectral entropy [17]	$O(N \log_2(N))$	Captures frequency domain information. Useful for analyzing signals in the frequency domain
Dispersion entropy [19]	$O(N^2)$	Sensitive to signal fluctuations and variations. Can reveal irregular patterns in the data
Attention entropy [18]	Varies	Depends on the specific attention mechanism used. Useful for capturing attention patterns in sequential data
Slope entropy [20]	$O(N)$	Measures the steepness of signal changes. Highlights abrupt transitions in the data

of all the entropy features dispersion entropy is capable of contributing the most to distinguish between normal and CI subjects (see Fig. 7) as it has the capability to recognize both time and frequency information along with simultaneous detection of noise. On the other hand Attention entropy also performed equally well by exploiting its technique to capture the most important frequency distribution of each PPG time series to identify its key patterns. Spectral entropy provided the list contribution amongst all due to the fact that it provides the broad power spectra of a given time series and thus miss the local information where most of the pathological changes correlated with CI can be captured.

5 Complexity analysis

Providing a complexity analysis of preprocessing and feature extraction is essential for making informed decisions, optimizing resource utilization, ensuring scalability and efficiency, and meeting real-world constraints in machine learning-based prediction systems. It contributes to the overall effectiveness and reliability of your machine learning solutions. We have used the combination of DWT and SG filtering in preprocessing stage. The following computational complexity of the proposed filtering approach with some of the other filtering approaches [6] is provided in Table 2. DWT filtering has a computational complexity of $O(N * log2(N))$, which is relatively efficient compared to other methods like moving average or median filtering (which can be O(N * M) or even $O(N * M * log2(M))$). Similarly, The computational complexity of SG filtering is O(N * M), which can be more efficient than some other methods for small filter sizes. Thus, the suggested filtering approach in the proposed work is computationally efficient and retains the clinical information of the PPG signals. Moreover, instead of dynamic filtering parameter we have chosen fix parameter for SG filter after investigation (frame length =61 and order=4) that brings more simplicity in preprocessing.

In feature extraction, the calculated entropies are chosen based on their potential to discriminate the PPG into two classes. Since the second and third derivative of PPG enhances the non-linear dynamics of PPG and increases their discriminative capabilities [12]. This property motivated us to use the non-linear features of the signal in terms of state-of-the-art entropy features. The computational complexity of each calculated entropy feature is mentioned in Table 3.

Dispersion entropy involves calculating various statistical measures, including variance and standard deviation, which are generally straightforward and computationally efficient. The simplicity of calculating attention entropy depends on the specific attention mechanism used. Some attention mechanisms can be relatively simple, while others involve more complex mathematical operations. Calculating slope entropy is relatively simple, primarily measuring the steepness of signal changes. This can be done by calculating the differences between consecutive data points. Calculating spectral entropy can be fairly complex, especially if you need to perform a Fourier transform to obtain the frequency domain representation of the signal. Overall, the calculation of these entropies is relatively simple compared to the other hybrid domain entropies. Moreover, we have yet to utilize any deep-learning model for prediction. Deploying classical regressor models is often more uncomplicated and straightforward than deep neural networks (DNNs) due to several key factors. Since they have relatively simple and interpretable structures, they consist of smaller parameters and well-defined mathematical equations, making them easier to understand and manage during deployment. Training classical models involves solving optimization problems with closed-form solutions, unlike DNNs that require iterative training using gradient-based optimization techniques, making the training process more complex. DNNs often demand significant computational resources, including powerful GPUs or TPUs, for training and inference. Classical models also benefit from well-established deployment tools and libraries. Hence, deploying the proposed prediction framework may be simple and efficient.

6 Conclusion

In this work, we proposed a machine learning-based automated framework for early prediction of cerebral infarction. We utilized four popular state-of-the-art entropy features to extract the CI pathology. The work has several merits, including PPG's key point independent approach, fewer features, and computationally simple design. In addition, we employed two-step PPG filtering in the preprocessing module to safely remove artifacts while retaining the natural PPG morphology. The experiment is done with PPG records for a limited number of subjects. Future work can involve multichannel PPG acquisition from a large population of CI and normal subjects. It can eliminate the feature engineering if the framework is developed with a deep neural network.

Funding This research did not receive any specific grant from funding agencies in the public, commercial, or not-for-profit sectors.

Declarations

Conflict of interest All authors declare that they have no conflicts of interest.

Ethical Approval Not applicable.

Consent to Participate Not applicable.

Consent to Publish Not applicable.

References

1. Donkor ES. Stroke in the century: a snapshot of the burden, epidemiology, and quality of life. Stroke research and treatment 2018 (2018).
2. Maruyama H, Tanahashi N. Diagnosis and treatment of cerebral infarction. Nihon rinsho Japanese J Clin Med. 2010;68(5):920–5.
3. Ave A, Fauzan H, Adhitya SR, Zakaria H. Early detection of cardiovascular disease with photoplethysmogram (PPG) sensor. In: 2015 international conference on electrical engineering and informatics (ICEEI), 2015;pp. 676-681. IEEE.
4. Gupta S, Singh A, Sharma A, Tripathy RK. DSVRI: a PPG-based novel feature for early diagnosis of type-II diabetes mellitus. IEEE Sens Lett. 2022;6(9):1–4.
5. Gupta S, Singh A, Sharma A. Exploiting moving slope features of PPG derivatives for estimation of mean arterial pressure. Biomed Eng Lett. 2022; 1-9.
6. Gupta S, Singh A, Sharma A, Tripathy RK. Exploiting tunable Q-factor wavelet transform domain sparsity to denoise wrist PPG signals. In: IEEE transactions on instrumentation and measurement, 2023;72, pp. 1-12. 4008012, https://doi.org/10.1109/TIM.2023.3287248.
7. Gupta S, Singh A, Sharma A. Dynamic large artery stiffness index for cuffless blood pressure estimation. In: IEEE sensors letters, 2022;6(3):1-4, 2022, 7000704. https://doi.org/10.1109/LSENS.2022.3157060.
8. Yu J, Park S, Kwon S-H, Cho K-H, Lee H. AI-based stroke disease prediction system using ECG and PPG bio-signals. IEEE Access. 2022;10:43623–38. https://doi.org/10.1109/ACCESS.2022.3169284.
9. Fallet S, Lemay M, Renevey P, Leupi C, Pruvot E, Vesin JM. Can one detect atrial fibrillation using a wrist-type photoplethysmographic device. Med Biol Eng Compu. 2019;57(2):477–87.
10. Eerikainen LM, Bonomi AG, Schipper F, Dekker LRC, de Morree HM, Vullings R, Aarts RM. Detecting atrial fibrillation and atrial flutter in daily life using photoplethysmography data. IEEE J Biomed Health Informat. 2020;24(6):1610–8.
11. Kulkarni TR, Dushyanth ND. Early and noninvasive screening of common cardio vascular related diseases such as diabetes and cerebral infarction using photoplethysmograph signals. Results Opt. 2021;3:100062.
12. Gupta S, Singh A, Sharma A, Tripathy RK. Higher order derivative-based integrated model for cuff-less blood pressure estimation and stratification using PPG signals. In: IEEE sensors journal, 2022;22(22):22030-22039. https://doi.org/10.1109/JSEN.2022.3211993.
13. Suboh MZ, Jaafar R, Nayan NA, Harun NH, Mohamad MSF. Analysis on four derivative waveforms of photoplethysmogram (PPG) for fiducial points detection. Front Public Health. 2022.
14. Liang Y, Liu G, Chen Z, Elgendi M. PPG-BP Database. figshare. (2018): Dataset. https://doi.org/10.6084/m9.figshare.5459299.v3
15. Singh BN, et al. Optimal selection of wavelet basis function applied to ECG signal denoising. Digital Signal Process. 2006;16(3):275–87.
16. Chatterjee A, Roy UK. PPG based heart rate algorithm improvement with butterworth IIR filter and Savitzky-Golay FIR filter. In: 2018 2nd international conference on electronics, materials engineering and nano-technology (IEMENTech), 2018; pp. 1-6. https://doi.org/10.1109/IEMENTECH.2018.8465225.
17. Zhang A, Yang B, Huang L. Feature extraction of EEG signals using power spectral entropy. In: 2008 international conference on BioMedical engineering and informatics, Sanya, China, 2008; pp. 435-439. https://doi.org/10.1109/BMEI.2008.254.
18. Yang J, Choudhary GI, Rahardja S, Franti P. Classification of interbeat interval time-series using attention entropy. In: IEEE transactions on affective computing. https://doi.org/10.1109/TAFFC.2020.3031004.
19. Rostaghi M, Azami H. Dispersion entropy: a measure for time-series analysis. IEEE Signal Process Lett. 2016;23(5):610–4.
20. Cuesta-Frau D. Slope entropy: a new time series complexity estimator based on both symbolic patterns and amplitude information. Entropy. 2019;21(12):1167.
21. McKight PE, Najab J. Kruskal-wallis test. The corsini encyclopedia of psychology 2010; p. 1.